

**ON THE ANALYSIS OF POST WELD HEAT TREATMENT RESIDUAL STRESS  
RELAXATION MECHANISM IN INCONEL ALLOY 740H BY COMBINING THE  
PRINCIPLES OF ARTIFICIAL INTELLIGENCE WITH THE EIGENSTRAIN  
THEORY**



Fatih Uzun<sup>1,2</sup>, Alexander M Korsunsky<sup>1,3,\*</sup>

<sup>1</sup>MBLEM, Department of Engineering Science, The University of Oxford

<sup>2</sup>fatihuzun@me.com, fatih.uzun@eng.ox.ac.uk

<sup>3</sup>alexander.korsunsky@eng.ox.ac.uk, \* corresponding author

Authors' Accepted Manuscript

Published version in *Materials Science & Engineering A*

Volume 752, 2019, Pages 180-191

<https://doi.org/10.1016/j.msea.2019.03.009>

## ABSTRACT

Post weld heat treatment (PWHT) process has an important role on fabrication of advanced ultra-supercritical power plant turbines. This process relieves the residual stresses formed as a result of welding by converting elastic strains into creep strains. In order to analyse the residual stress relief mechanism during the PWHT process, a novel simulation approach based on experimental data was developed for the analysis of residual stress states from complex manufacturing processes which are welding and heat treatment. This model uses permanent plastic strains (eigenstrains) formed as a result of welding process to set the initial mechanical state of the sample. The distribution of eigenstrains in the whole body was determined using displacement data obtained from contour measurements. The use of eigenstrains to set the initial residual stress state of the creep model reduced the number of uncertainties. This allowed the use of the principles of artificial intelligence for the development of a new fuzzy finite element model (fFEM) that determines the eigenstrain-creep model parameters through an evolution process. Subsequent to the determination of the model parameters, conditions of the PWHT process are investigated to analyse residual stress relaxation mechanism in Inconel Alloy 740H weldments.

**Keywords:** volumetric residual stress; post weld heat treatment; eigenstrain-creep model; artificial intelligence; fuzzy finite element model; evolutionary algorithms

## NOMENCLEATURE

$\dot{\varepsilon}_e'$	rate of elastic strain relaxation
$\dot{\varepsilon}_{cr}$	rate of uniaxial equivalent creep strain

$\varepsilon_e'$	relaxed elastic strains
$c_0$	coefficient of thermal expansion at base temperature
$M_j$	mutation search range
$p_{(+)}$	factor for expansion of $p$
$p_{(-)}$	factor for reduction of $p$
$P_B$	base population
$P_N$	new population
$V_j$	$j^{th}$ gene of vector of model parameters
$\{V\}$	vector of all model parameters
$X_i$	measured and averaged displacement
$Y_i$	calculated displacement
$\varepsilon_{e_0}$	total of elastic strains formed by eigenstrains
$\varepsilon_{cr}$	total of uniaxial equivalent creep strains
$\varepsilon_p$	total of eigenstrains
$a$	number of measurement points
$B$	constant of the power-law relation
$c$	coefficient of thermal expansion
$f$	mean squared error
$k$	Boltzmann's constant
$m$	constant of the power-law relation
$n$	constant of the power-law relation
$p$	mutation range constant
$q$	constant of the power-law relation ( $Q/k$ )
$Q$	creep activation energy
$T$	temperature

$t$	total time
$u$	constant for coefficient of thermal expansion calculations
$u$	a constant for temperature dependence of CTE
$\sigma$	equivalent stress

## 1. INTRODUCTION

Components used in aerospace industry includes nickel-based age hardened super-alloys because of their high resistance to creep and corrosion and weldability at high temperatures [1]. Being able to operate at high temperature and pressure conditions successfully made super-alloys a candidate for advanced ultra-supercritical (A-USC) power plants. Inconel Alloy 740H is a super-alloy designed for using in A-USC power plants and it has ASME Code Case 2702 that allows it to be used for welded construction [2]. Performance of this alloy was investigated in the recent studies. Patel et. al. [3] performed experiments to investigate corrosion resistance, mechanical properties and weldability. Creep rupture reduction of Inconel Alloy 740H welds were investigated by Bechetti et. al. [4] by performing metallographic analysis of the microstructural changes during creep. Studies showed that Inconel Alloy 740H meets design requirements for power plant components [5], however welding and subsequent heat treatment during have negative influence on creep properties of this precipitation hardenable superalloy.

Properties, reliability and operation behaviour of the materials used for steam turbine components are influenced by the welding process. According to the report of Cerjak [6], this process has various applications during fabrication and operation. Most common uses of welding process are joining of components and repairing the damages, but this process causes

internal stresses to be risen. Various methods can be used to measure welding residual stresses which are diffraction [7], contour [8] and ultrasonic [9–11] methods. However, diffraction methods are expensive, contour methods are destructive and ultrasonic waves are not able to grasp necessary sensitivity.

Masubuchi [12] stated that the use of computers for the purpose of weld modelling dates back to 1960s. Advancements on the computation power during the decades allowed the development of numerical models for understanding the mechanism behind formation of welding residual stress. Thermal elastic plastic, inherent strain and inverse eigenstrain methods were all developed as numerical models. Inverse eigenstrain method combines benefits of numerical simulations with experimental data obtained by X-Ray and neutron diffraction or contour measurements. DeWald and Hill [13] used contour measurements for determination of eigenstrain distribution to reconstruct volumetric residual stresses and several other examples of this method can be found in the book of Korsunsky [14].

Residual stresses have harmful effects on the properties and operating conditions of materials. Yan et. al. [15] stated that post weld heat treatment (PWHT) is a common method used for reduction of residual stresses and improvement of mechanical properties. Studies on Inconel 718 super-alloys [16,17] showed that metallurgical and mechanical properties of super-alloys are directly influenced by PWHT process. In order to get materials with requested properties, parameters of the PWHT process should be determined carefully. Testing the materials before and after the PWHT can help to understand the effect of process parameters but large-scale and expensive industrial components turns this demand into a challenging task.

According to Saunders [18] residual stresses in viscoelastic materials relaxes when subjected to constant strain which can be ensured by thermal strains and the role of creep on relaxation of residual stresses during PWHT process was presented by Yan et. al. [15]. Comparison of creep and thermal expansion only models supported the influence of creep on residual stress relief. There are three creep models commonly used for simulating PWHT process which are Norton, Norton-Bailey and Omega models. Previous studies performed using these models can be found in the papers of Berglund et. al. [19], Takazawa and Yanagida [20] and Dong et. al. [21] respectively. Among these models, Norton-Bailey Law allows investigation of both transient and steady state creep behaviours.

Simulation of welding process and PWHT process is a challenging task that requires precisely determined temperature dependent material properties and consumes high amount of computation power. Classical approach of finite element simulation of PWHT process comprises subsequent thermal and structural analyses. Josefson [22] performed one of the first attempts for finite element modelling of residual stress relaxation. Improvements in the computation technology allowed development of a fully coupled thermal-mechanical analyses for investigation of residual stresses after welding and PWHT processes by Berglund et. al. [19]. Alberg and Berglund [23] simulated stress relief heat treatment process and stated that Norton creep law should be preferred because of its simplicity and accuracy. Yaghi et. al. [24] performed finite element simulation of PWHT process using Norton creep law whose parameters are calculated using the data from stress relaxation tests. Residual stress mitigation was estimated by Takazawa and Yanagida [20] through a thermal elastic plastic creep procedure using both Norton and Norton-Bailey laws. A coupled thermal-mechanical analysis was performed by Venkata et. al. [25] to study PWHT and its parameters to have optimum residual stress relaxation. Dong et. al. [21] used a thermal mechanical model to analyse

different PWHT condition on relaxation of welding residual stress. Another study that analyses PWHT conditions was conducted by Yan et. al. [15]. Authors used Arrhenius equation based creep model to include effect of temperature, stress state and time in their calculations. As a summary, current models that aims understand the role of creep during PWHT on residual stress relief are based on thermal elastic plastic mechanical models and creep calculations are done using Omega, Norton, Norton-Bailey or Arrhenius creep models. However, the quality of elastic plastic model consumes high computation power and the accuracy of simulations are limited to the quality of thermo-mechanical material properties. Effect of creep on microstructure of Inconel Alloy 740H fusion welds previously investigated by Bechetti [4]. Authors performed microscopic analyses and creep rupture tests to understand the reduction of creep rupture behaviour and related microstructural changes. In a later study, Uzun and Korsunsky [26] investigated the main source of welding residual stress by solving inverse eigenstrain problem using Inconel Alloy 740H fusion welds with bead-on-plate specimen design. Comparison of as-welded and post weld heat treated models showed the effect of creep during the PWHT process on residual stresses. There are other studies found in the literature devoted to materials designed for ultra-supercritical power plants, but they do not provide information about the creep behaviour and its role in residual stress relief during the PWHT process.

Numerical simulations require determination of model parameters properly. However, limited number of trials for the determination of model parameters always have a risk of missing the global optimum among infinite number of alternative solutions. In order to deal with this problem, artificial intelligence (AI) based methods are being developed. Russel and Norvig [27] stated that AI is the study and design of intelligent agents. In the case of solving complex

engineering problems, an intelligent agent can be the model designer or an artificial agent. AI based smart models replace the model designer with an artificial agent.

Quiza et. al. [28] classified the methods that combine AI and FEM as FEM/AI, AI/FEM, Hybrid and fuzzy FEM models. Fuzzy FEM models are based on updating uncertain design parameters and material properties of a core finite element model. Moens and Vandepitte [29] concludes that the solution strategy should be determined according to deterministic or non-deterministic property of the finite element model. Global optimization procedures can be used for determination of the optimum model parameters while the core is a deterministic finite element model.

The quality of creep calculations is always questionable because, in spite of the fact that stress fields in mechanical systems are inhomogeneous, uniaxial stress fields created in rods are used for the determination of creep rate [30]. The difficulty on modelling of creep mechanism of metals was discussed by Bratke and Josefson [31] and authors proposed a method for determination of parameters of Norton-Bailey Law. Based on these facts, it can be stated that the determination of creep properties for a specific material is still a challenging task. In order to deal with this problem, principals of the artificial intelligence are used to develop a fuzzy finite element model for determination of creep properties of Inconel alloy 740H.

Plastic behaviour of super-alloys has been studied but comprehensive models to analyse creep behaviour of these materials during the PWHT processes are still missing. In the present study, an artificial agent was developed as a fFEM model to calculate the creep-induced residual stress relaxation. During the development of the fFEM, the contour method was enhanced with the introduction of eigenstrain-based modelling. This provided clear



identification of the sources of residual stress (misfit strain), their nature and distribution. Secondly, it was discovered that the identification of the domain where eigenstrains exist can be best accomplished by using genetic algorithms. Thirdly, we investigated and drew conclusions regarding the nature of stress relaxation during heat treatment, that is driven by the modification of eigenstrain sources of residual stress. Overall, that means that we are reporting a coherent approach to the analysis of residual stress states from complex manufacturing processes (welding + heat treatment) supported by simulation validated through comparison with experimental data. The fFEM determined the optimum model parameters through an evolutionary optimization process that minimizes the MSE between calculated and experimentally measured displacements. After the determination of model parameters, the core deterministic finite element creep model, which is called as eigenstrain-creep model, was used for the analysis of PWHT process conditions in terms of ambient temperature and holding time.

## **2. MATERIALS**

As-welded and heat-treated specimens of Inconel Alloy 740H are machined according to the geometric properties given in Figure 1. This is a bead-on-plate specimen design which has weld bead placed on the top of the plate. The reason for selecting this design is investigating different stages of the welding process. Centre of the cartesian coordinates is located at the centre of yz plane at the bottom of the plate. The specimen thickness is 12 mm and its length and width are 200 and 150 mm, respectively. The weld slot width was determined to be 12 mm and its length 67 mm. The depth of the weld slot was 5 mm and the width and the length at the deepest section were 8 mm and 63 mm respectively.

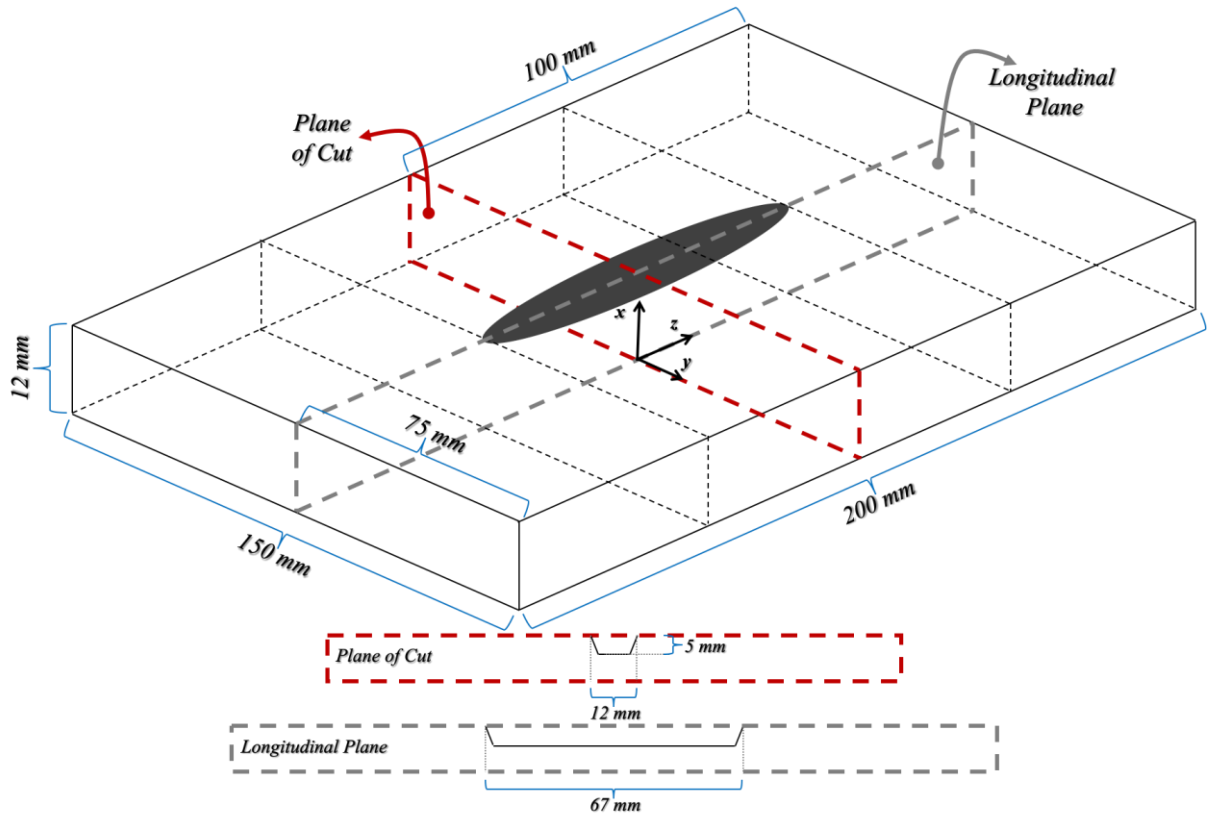


Figure 1. Representation of dimensions of Inconel Alloy 740H specimens

The nominal chemical composition of the plate and the filler material can be found in the data sheet provided by Special Metals Corporation [5]. The elastic modulus of the specimen was determined to be 221 GPa from this data sheet. Subsequent to the machining of the weld slots, specimens were pre-weld annealed at 1107 °C for 1 hour and water cooled. Three weld beads are applied to two specimens using tungsten inert gas (TIG) welding technique. The parameters of this welding process are given in Table 1. One of the welded specimens is post-weld heat treated (aged) at 800 °C for 4 hours followed by air cooling. Electron discharge machining (EDM) technique is used for cutting both as-welded and post-weld heat treated specimens from the plane of cut which is illustrated in Figure 1.

Table 1. Parameters of TIG welding process

	Weld Pass 1		Weld Pass 2		Weld Pass 3	
	AW	HT	AW	HT	AW	HT
Current (A)	174.0	174.0	174.0	174.0	174.0	174.0
Voltage (V)	16.1	16.0	16.3	16.5	16.3	16.2
Travel Speed (mm/min)	163.0	136.4	152.4	111.5	134.3	123.4
Wire Speed (mm/min)	177.8	254.0	228.6	304.8	177.8	228.6

### 3. CALCULATION OF RESIDUAL STRESSES

Residual stresses are the stresses that are accommodated in a material without any external load. Determination of these stresses is a challenging task while understanding their distribution in a material has vital importance. Ahn et al. [32] states that it is impossible to get a full map of six components of residual stress in engineering components using currently available expensive and time-consuming methods. For this purpose, thermal elastic plastic finite element models are widely used but these models require careful determination of heat source geometry, temperature dependent material properties and dimensions of the material. When the complexity of plasticity and details of thermal model are included, high number of unknowns causes the results of these models to highly deviate from experimental validations. In order to deal with difficulties, the contour [33] and the eigenstrain-contour [8,13,26] methods are developed to combine experimental data with numerical models. In this study, both of these methods are used for experimental validation and determining initial mechanical conditions of the eigenstrain-creep model.

### **3.1. The Contour Method**

According to the principle of superposition, residual stresses relax elastically, and they can be correlated with deformations formed as a result of stress relaxation. The contour method uses deformations on a planer cut appeared after EDM sectioning process and combines experimental measurements with an elastic finite element model to quantify residual stress distribution on the surface of cut. Finite element model simulates the conditions before the cutting process using the inverse of processed displacement data. Reliable results of the simulation are limited to the stresses normal to the plane of cut. In this study, contour method is used for calculation of experimental residual stresses for validation of simulation results. The same procedure of contour method, which is explained in the previous studies of present authors [26,34,35], is applied for experimental determination of displacements and residual stresses. Distribution of the processed displacement data can be found in the paper that investigates the eigenstrain sources of welding residual stress [26]. Accordingly, results of the contour method calculations of this study for as-welded and heat-treated specimens are the same with that study.

### **3.2. The Eigenstrain-Contour Method**

Eigenstrain-contour method combines accuracy of high-density experimental data from contour measurements with elastic finite element models for reconstruction of eigenstrain fields and calculation of residual stresses corresponding to the eigenstrains. The idea behind this approach is using the main source of residual stresses, permanent plastic strains, which are called as eigenstrains. This method is first introduced by Mura [36] in 1981. Korsunsky [14] presented examples of this method in various applications and recent studies showed that

iterative calculations and the use of principles of artificial intelligence allow determination of volumetric residual stresses and distortions in large scale welded components [26,34,35].

Previously it was shown that the main source of welding residual stress is the eigenstrains in and around the weld beam [26]. Authors analysed three different models for solving inverse eigenstrain problem. Formulation of these models and results of the analyses can be found in that paper. Among these models, multi-component iterative model provided effective results with a high quantified quality of fit in terms of mean squared error (*MSE*). In this study, the same iterative solution process is used to determine the eigenstrain sources of the residual stress in as-welded specimen of Inconel alloy 740H.

#### **4. SIMULATION OF PWHT PROCESS**

Modelling of creep behaviour of welded structures and simulation of PWHT process require thermo-mechanical calculations for determination of welding residual stresses. Precision of these calculations is directly related with the quality of temperature dependent material properties. Accordingly, the creep models based on elastic-plastic calculations include high number of parameters that increase uncertainty of the model. On the other hand, determination of eigenstrain distribution in a body turns calculation of residual stress fields into a linear elastic problem that eliminates the uncertainties related to the elastic-plastic calculations. Linear-elastic calculations of the eigenstrain-contour method reduces the computation cost drastically when compared to elastic-plastic calculations and the use of experimental data for reconstruction of residual stress fields provides highly reliable results. The eigenstrain sources of residual stresses in a weldment can be used to simulate PWHT process but this does not eliminate the requirement of temperature dependent material

properties for creep calculations. The principles of artificial intelligence herein can be used for the determination of parameters of a creep model using an artificial agent [35]. In this study, experimental data from contour measurements are used in a fFEM for the purpose of determination of parameters of eigenstrain-creep model based on Norton-Bailey creep law.

#### **4.1. The Eigenstrain-Creep Model**

Based on the fact that holding stressed materials at elevated temperatures for sufficiently enough time causes elastic strains to convert into plastic strains, PWHT process allows relaxation of welding residual stresses [37]. Accordingly, creep, which is a time dependent deformation that takes place in metals after prolonged exposure to stress at elevated temperatures, is regarded as the driving mechanism of PWHT process [38]. Dong et. al. [21] and Yan et. al. [15] verified this mechanism by comparing thermal expansion and creep based independent models of PWHT process.

Betten [39] explained that Norton and Bailey [40,41] developed a constitutive model to predict time-dependent inelastic deformations that occur in primary and secondary creep stages. The power-law relation that defines the uniaxial equivalent creep strain rate,  $\dot{\epsilon}_{cr}$ , is given in Equation 1 below, where  $B$ ,  $n$  and  $m$  are constants specific to the material and process conditions,  $\sigma$  is the equivalent stress and  $t$  is the total time. This formulation is also called as time-hardening creep model which is preferred to be used for prediction of creep histories at constant stress and temperature conditions [42].

$$\dot{\epsilon}_{cr} = B\sigma^n t^m \quad (1)$$

Creep mechanism is based on the movement of dislocations when the stress state is high. Pelleg [43] stated that dislocation glide can occur at low and high temperatures and besides, self-diffusion and creep activation energies are almost the same. For this reason, temperature dependence of creep laws can be applied to the creep models by Arrhenius law [44]. The modified creep rate relation that include Arrhenius relation is given in Equation 2, where  $Q$  is creep activation energy,  $k$  is Boltzmann's constant, and  $T$  is temperature. In this equation,  $Q/k$  is replaced by a new constant,  $q$ , in eigenstrain-creep model calculations.

$$\dot{\varepsilon}_{cr} = B\sigma^n t^m \exp(-Q/kT) \quad (2)$$

The eigenstrain-creep model for simulation of PWHT process calculates relaxation of welding residual stresses which are imported to the creep model in terms of eigenstrain. In this simulation the rate of change of eigenstrain is equal to zero. Jeong et. al. [45] stated that the rate of formation of plastic creep strains,  $\dot{\varepsilon}_{cr}$ , is equal to the rate of relaxation of elastic strains,  $\dot{\varepsilon}_e'$ . Accordingly, the total strain at time  $t$  of PWHT process can be expressed in terms of initial elastic strains,  $\varepsilon_{e_0}$ , relaxed elastic strains,  $\varepsilon_e'$ , eigenstrains,  $\varepsilon_p$ , and plastic creep strains,  $\varepsilon_{cr}$ , using Equation 3.

$$\varepsilon_{tot} = \varepsilon_{e_0} - \varepsilon_e' + \varepsilon_p + \varepsilon_{cr} \quad (3)$$

#### 4.2. The Fuzzy Finite Element Model

The quality of creep calculations is always questionable because, in spite of the fact that stress fields in mechanical systems are inhomogeneous, uniaxial stress fields created in rods are used for the determination of creep rate [30]. The difficulty on modelling of creep mechanism

of metals was discussed by Bratke and Josefson [31] and authors proposed a method for determination of parameters of Norton-Bailey Law. Based on these facts, it can be stated that the determination of creep properties for a specific material is still a challenging task. In order to deal with this problem, principals of the artificial intelligence are used to develop a fuzzy finite element model for determination of creep properties of Inconel alloy 740H.

The simulation of PWHT process requires elastic properties for elastic-plastic calculations and creep properties and coefficient of thermal expansion (CTE) for creep calculations.

Thermal analysis is performed using thermal properties of the Inconel Alloy 740H obtained from the study of DeBarbadillo [46] to determine the thermal history of PWHT process.

Temperature dependence of (CTE) is determined using Equation 4,  $c$ , where  $u$  is a constant specific to the model, that determines the linear relation of the CTE with respect to temperature, and  $c_e$  is the CTE at base temperature which is set to  $12 \mu\text{m}/\text{m}^\circ\text{C}$ .

$$c = c_0(1.0 + uT) \quad (4)$$

Eigenstrain-creep model has four parameters. The inclusion of temperature dependence of CTE increased the total number of model parameters to 5. The vector that includes all model parameters is given in Equation 5.

$$\{V\} = \{B, n, m, q, u\}^T \quad (5)$$

The aim of fFEM is acting as an intelligent agent for the determination of the model parameters in a way to get best fit between PWHT simulation results and experimental data obtained from post weld heat treated specimen. Several artificial intelligence tools have been



developed for solving engineering problems. Quiza et. al. [28] classified metaheuristic optimization methods as one of the artificial intelligence methods. Simple genetic algorithm is a subset of evolutionary algorithms which is inspired from the evolution process. In this study, artificial agent uses basic rules of genetic algorithms to determine optimum model parameters. The mean squared error (MSE) between experimental and calculated displacements is the objective function of this process which is given in Equation 6 where  $Y_i$  is the calculated and  $X_i$  is the measured and averaged displacement value in the  $i^{th}$  measurement point and  $a$  is the total number of measurement points.

$$f = \frac{1}{a} \sum_{i=1}^a (Y_i^2 - X_i^2) \quad (6)$$

Zero-order optimization schemes allow solution of complex problems in the cases of the lack of explicit function. The eigenstrain-creep model includes 8 parameters, but there is not a mathematical formulation that combin these parameters. Accordingly, it was necessary to use a zero-optimization method to define optimum model parameters. Among other metaheuristic search methods, evolutionary algorithms has proven advantages which are discussed by Fogel [47]. Their capability for self-optimization and being able to solve problems that have no known-solutions [47] eliminate the requirement of a human intervention. These properties of evolutionary algorithms make genetic algorithms an appropriate method for developing an artificial agent.

Flow chart of the binary genetic algorithm process is given in Figure 2. The process starts with generation of initial population which is called as the base population,  $P_B$ . The number of members in a population is determined to be 5. Each member of the population is composed of 5 model parameters which are determined randomly around initial parameters, which are

given in Table 2, within predetermined search range. Initial population is evaluated by solving the core deterministic eigenstrain-creep model and applying operators of simple genetic algorithms, which are elitism, selection, crossover and mutation, to generate new population,  $P_N$ . The best member of the population is determined as the elite member and it is transferred to the next generation. Selection of members for single point crossover is performed using pie-graph method [48]. Crossover is performed with a probability of 0.5 and it is followed by mutation of genes of non-elite members with 0.95 probability. After the evaluation of the new population, best solutions of the base and the new populations are compared to make a decision on mutation search range,  $M_j$ . Mutation search range of  $j^{th}$  gene is expanded or reduced by modifying the mutation range constant,  $p$ , using Equation 7. This constant is initially set to 0.1. If the new population has better MSE than base population, the mutation range constant is expanded by multiplying by  $p_{(+)}$ , otherwise it is reduced by multiplying with  $p_{(-)}$ .  $p_{(+)}$  and  $p_{(-)}$  are determined to be 1.1 and 0.9 respectively and kept constant throughout the evolution process. Finally, the termination criterion is checked and a new generation is created or the process is ended. Previously, a similar procedure was successfully applied by Toklu and Uzun [49], Uzun [50,51] and Uzun and Korsunsky [35] to find global optimum for solving engineering problems.

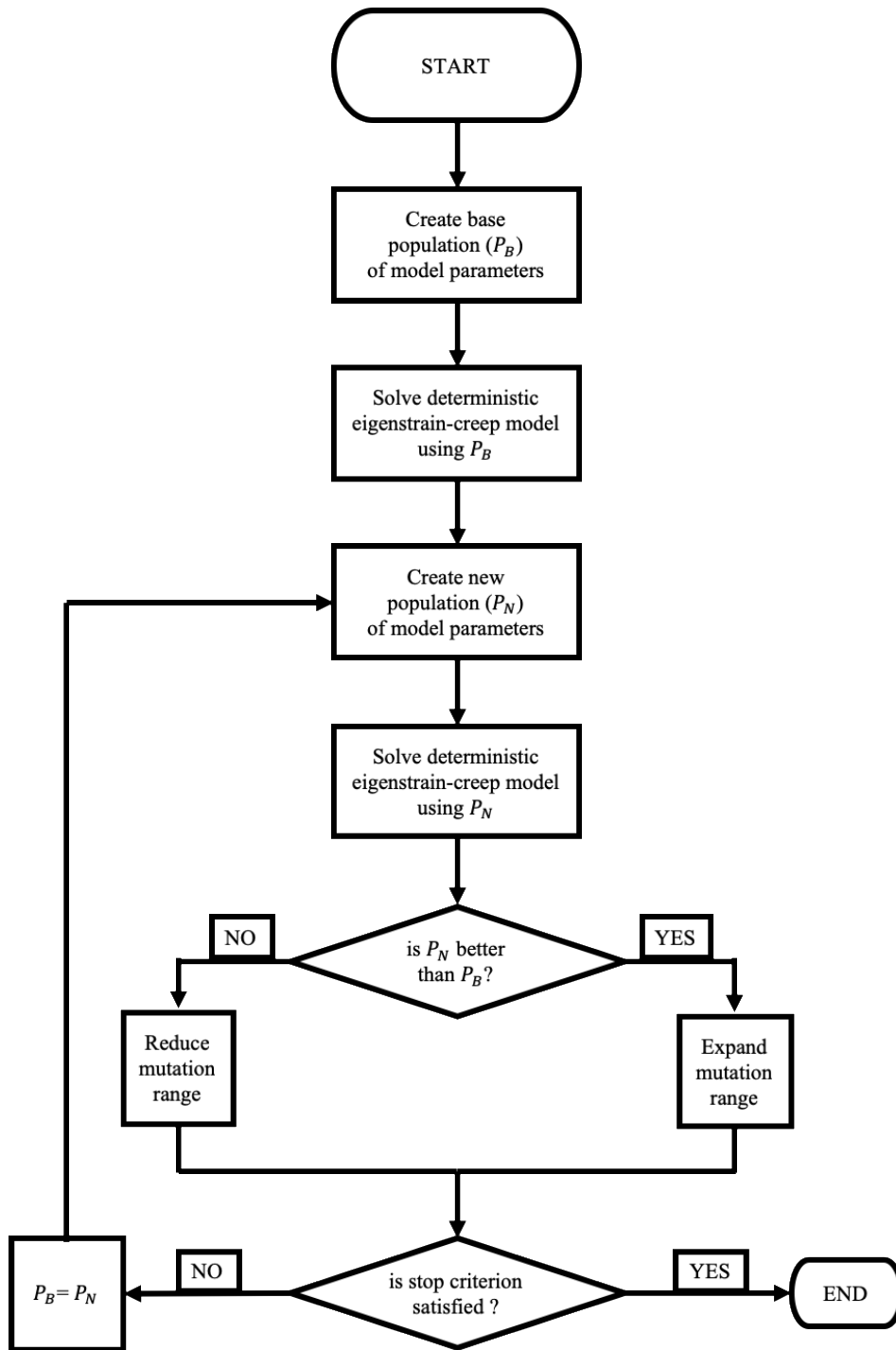


Figure 2. Flowchart of the fuzzy finite element model for the determination of eigenstrain-creep model parameters

$$M_j = V_j p \quad (7)$$

In this study, fFEM model is created as a Python script for ABAQUS 6.14-5 commercial finite element solver. The model calculations are performed in a computer with Intel® Core™ i7 processor that has 4 physical cores. Mesh density is determined in a way to create a balance between solution time and accuracy of the solution. The cuboid model geometry is meshed by C3D8R general purpose brick element. This element has reduced integration point. Trials showed that the number of elements above 13720 does not provide a significant improvement in the solution accuracy. Therefore, the mesh density is limited by that number of elements. The model is accepted to be symmetric at the plane of cut. Accordingly, symmetry boundary condition is applied on the surface where experimental surface displacements are applied in eigenstrain-creep model. The contour and the eigenstrain-contour methods use experimental surface displacements to calculate residual stresses, but these models do not use a symmetry boundary condition.

## **5. RESULTS**

The proposed method is based on subsequent solution of two models that use experimentally determined out-of-plane displacement data obtained from the EDM-cut surface of as-welded and heat-treated specimens. The first model calculates residual stresses in the welded specimen by solving inverse eigenstrain problem. The second model simulates PWHT process using the eigenstrain distribution obtained using the first model. Both of the models use symmetric half of the bead-on-plate specimen design. In this study, high density and accuracy of the contour measurements increased the reliability of the model results. The experimental displacement data sets were used to determine residual stresses on the surface of EDM-cuts using the contour method for experimental validation of the eigenstrain-contour and the eigenstrain-creep model results.

### 5.1. Contour and Eigenstrain-Contour Models

Multi-component iterative solution determined the eigenstrain distribution that provide best fit of displacements. Results show that eigenstrains that cause formation of residual stresses are collected in and around the weld zone as illustrated in Figure 3. Front face of the illustration represents symmetry plane of the plate. Both components of eigenstrain have the same distribution. The ratio between them is determined based on the assumption that  $zz$  and  $yy$  components of eigenstrain are proportional with a fixed coefficient. Details of the iterative solution to determine the fixed coefficient can be found in the pre-mentioned study of the authors.

Profile distributions of through-thickness averages of displacements and residual stresses, corresponding to the eigenstrain fields given in Figure 3, are illustrated in Figure 4. Results of the eigenstrain model have a good agreement with experimental results. Validated distribution of eigenstrain components is transferred to the second model for simulation of the PWHT process.

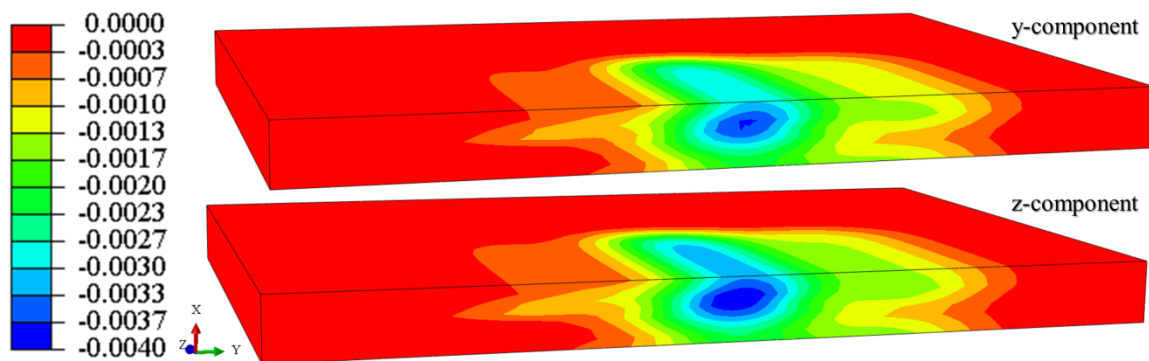


Figure 3. Distribution of eigenstrains in terms of temperature in as-welded model [26]

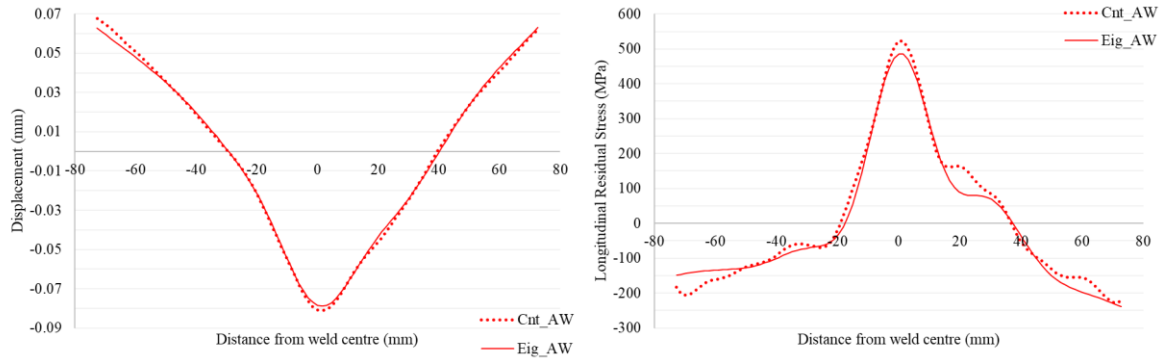


Figure 4. Comparison of the through-thickness average of displacements (left) and residual stresses (right) on the surface of cut determined using the eigenstrain-contour method and the contour method

## 5.2. fFEM and Eigenstrain-Creep Model

Eigenstrain-creep model for the simulation of PWHT process used on eigenstrain fields determined for aw-welded specimen. The thermal history of the PWHT was determined using a thermal transient finite element model that includes conductive and convective terms of heat transfer. This finite element model simulated heating up to 800 °C, holding at that temperature and cooling at room temperature. Three stages of this process is illustrated in Figure 5.

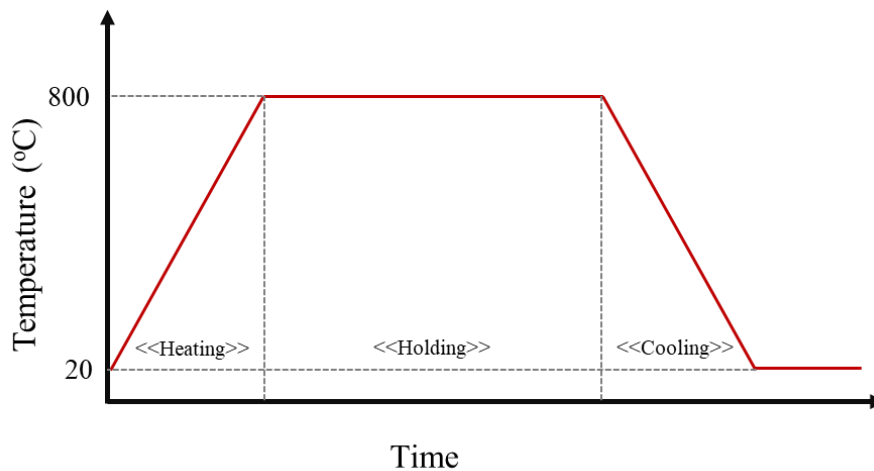


Figure 5. Three stages of PWHT process

fFEM started with roughly estimated initial parameters given in Table 2. After 20 generations, the algorithm has been stabilized as illustrated in Figure 6. Proceeding 10 generations did not provide any more improvement and the process was ended after satisfying the termination criterion. The proposed algorithm expands or reduces the mutation range after each generation. The termination criterion is based on this property of the algorithm. After 30 generations, the mutation range was reduced up to the limit determined for termination. The optimum set of parameters that provide the best fit of displacement with the experimental displacement measurements form post weld heat treated specimen are given in Table 2. Total number of solutions after 30 generations is 150. Solution time is minimized by parallelization option of ABAQUS using Intel i7 CPU. Each solution of eigenstrain-creep model lasted about 5 minutes.

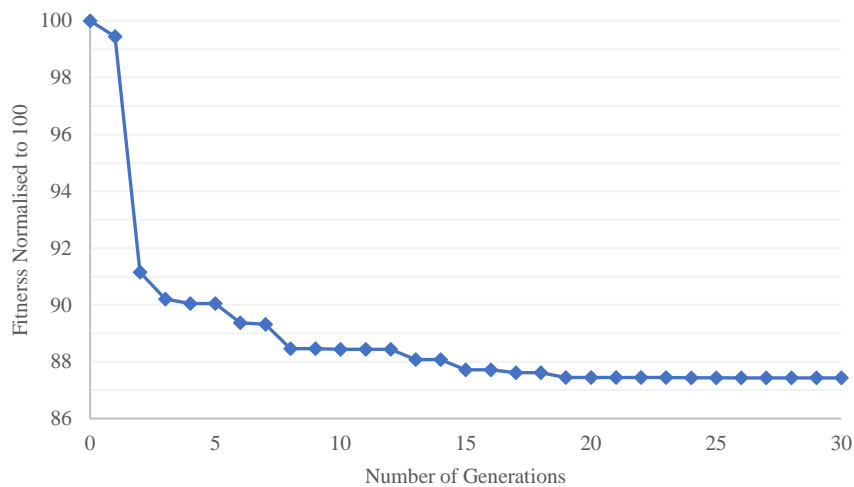


Figure 7. Normalised values of fitness function during the evolution of the fFEM

Table 2. Initially predicted and final parameters of fuzzy finite element creep model

	$B$	$n$	$m$	$q$	$u$
Initial	$2.0 \times 10^{-13}$	3.0	-0.3	-800.0	-0.0003
Final	$1.94077 \times 10^{-13}$	2.81063	-0.26614	-924.4035	-0.00033755

Solution of the eigenstrain-creep model calculated the stress relaxation after PWHT process. Comparison of the profile distribution of the through thickness averaged longitudinal residual stresses from experimental contour method measurements and creep model calculations are given in Figure 8. Distribution of remaining residual stresses after stress relaxation shows good agreement with contour method calculations. The fuzzy finite element creep model determined almost the best solution in terms of MSE, although, the agreement is not as good as it is in eigenstrain reconstruction of as-welded specimen. This is because the experimental results of the heat-treated conditions were obtained from a different specimen in spite of the fact that it was machined and welded under the same conditions with the as-welded specimen.

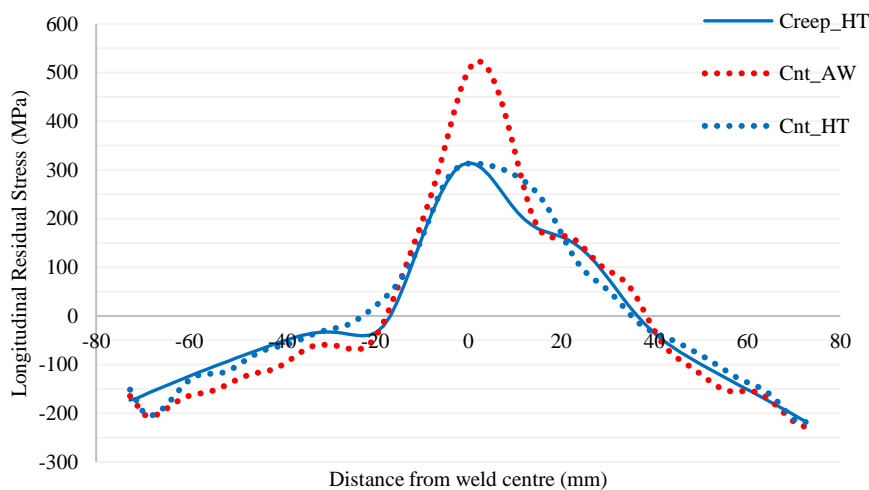


Figure 8. Transversal profile distribution of the through-thickness average of longitudinal residual stresses on the surface of cut calculated using the eigenstrain-creep model and the contour method



Time histories of temperature, longitudinal residual stress and longitudinal creep strain of the single solution obtained using the optimum model parameters, which were measured from a single point 5 mm below the top in the centre of symmetry plane (analysis point), are given in Figure 9. Creep strain increases during the heating, the holding and initial period of the cooling stages. Residual stress decreases until the end of holding period. During the rapid decrease of temperature, residual stress increases up to a point less than its initial value. In order to understand different PWHT conditions of Inconel Alloy 740H, effect of ambient temperature and holding time are analysed using the eigenstrain-creep model with optimum set of parameters.

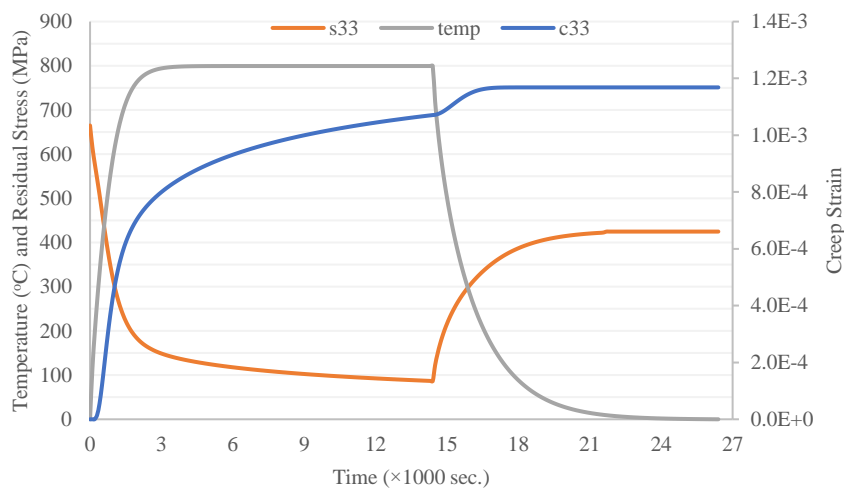


Figure 9. Time histories of temperature, longitudinal residual stress (s33) and longitudinal creep strain (c33) of the single solution obtained using optimum model parameters

### 5.3. Effect of Ambient Temperature

The eigenstrain-creep model with the optimum parameters was used to analyse the effect of ambient temperature on the PWHT process. Five different temperatures were tested from 200 to 1000 °C. Thermal histories of each process can be found in Figure 10. Holding time is the

same for all solutions. Time histories of longitudinal creep strain and longitudinal residual stress at the analysis point are illustrated in Figures 11 and 12. Results show that maximum creep strain is achieved when the ambient temperature is 400 °C. Residual stress relaxation appeared to show good agreement with the creep strain results, with greatest residual stress reduction achieved at 400 °C. On the other hand, stress relaxation during the holding period is directly proportional with the ambient temperature. Highest relaxation is achieved when the ambient temperature is 1000 °C. However, residual stresses are recovered during the cooling stage. Residual stress recovery during this stage is proportional with the temperature. Higher ambient temperature results with higher residual stress recovery.

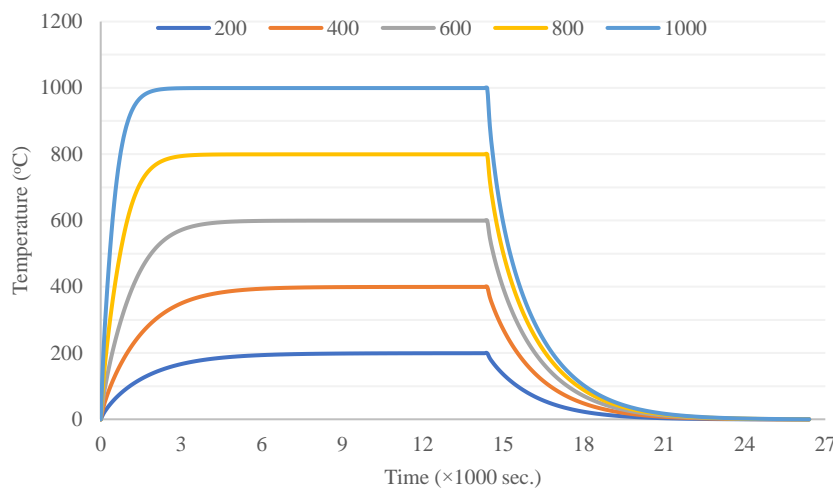


Figure 10. Thermal histories of solutions at different ambient temperatures

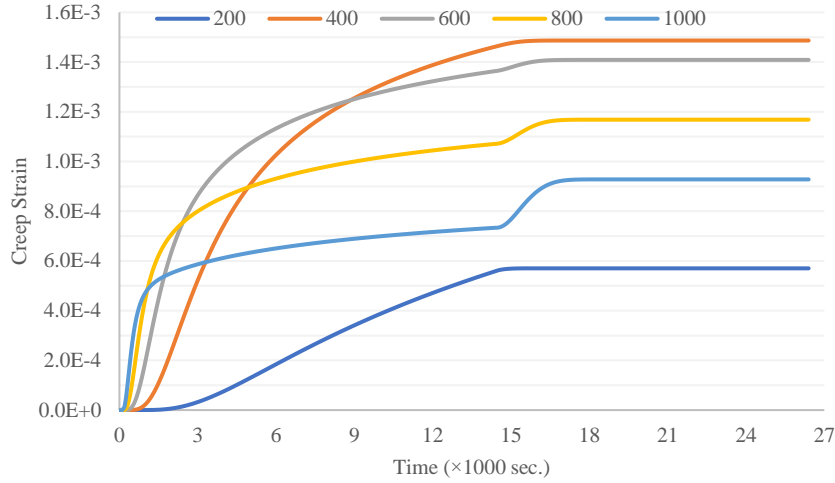


Figure 11. Time history of longitudinal creep strain at different ambient temperatures

Final creep strain and residual stress values at the end of PWHT at the analysis point are illustrated in Figure 13. Results show that the recovery during the cooling period has a high influence on final residual stress. In order to achieve better residual stress relaxation, different cooling plans can be designed, but this issue is out of scope of this paper. According to the results illustrated in Figure 12, it can be stated that, the optimum stress relaxation can be achieved at an ambient temperature around 400 °C.

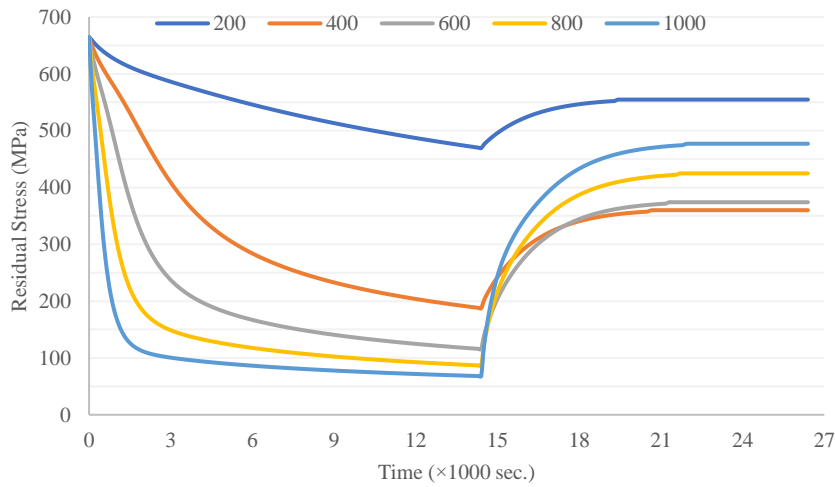


Figure 12. Time history of longitudinal residual stress at different ambient temperatures

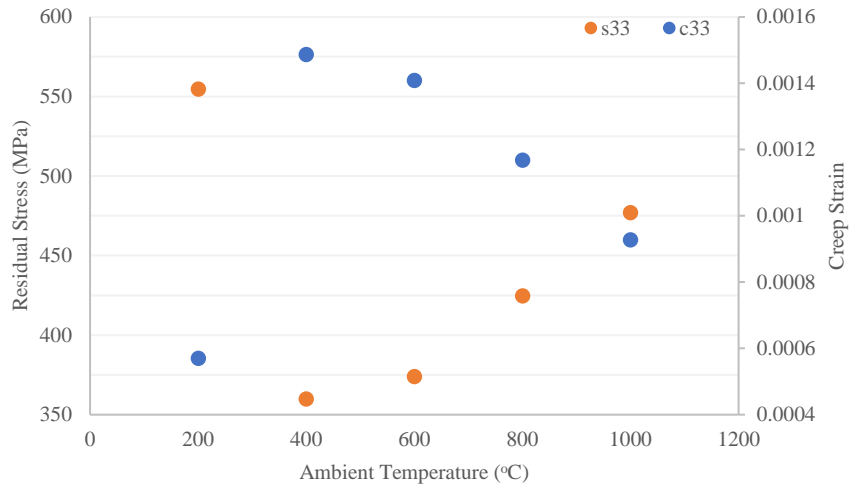


Figure 13. Final creep strain and residual stress values at the end of PWHT process at five different ambient temperatures

#### 5.4. Effect of Holding Time

The effect of holding time on the residual stress relaxation is analysed using six different solutions performed at holding times varying from 1 to 6 hours. Thermal histories of solutions with all holding times are given in Figure 14. Cooling time for all solutions are the same.

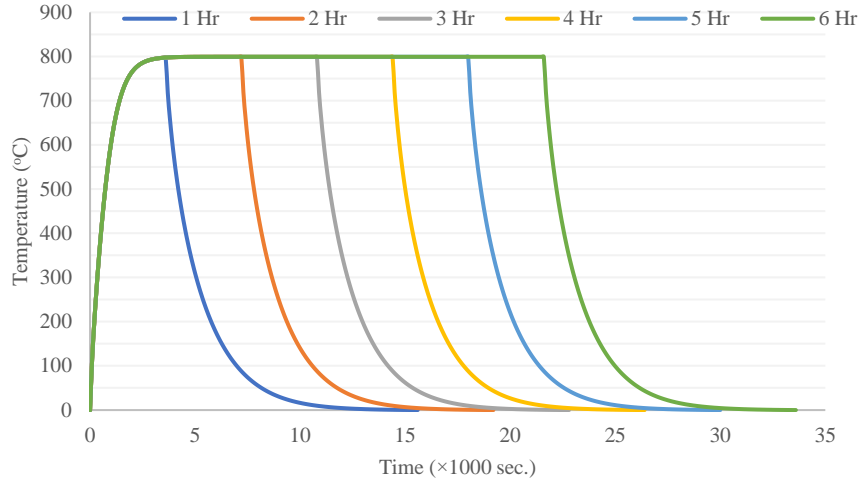


Figure 14. Thermal histories of solutions at different holding times

Time histories of longitudinal creep strain at the analysis point for all solutions are illustrated in Figure 15. Results show that the holding time has an influence of the magnitude of creep strain. Increasing the holding time increases the creep strain but the difference at each step gets lower with the increase of holding time. Residual stress time histories at the analysis point show that holding time has a minor effect on the residual stress relaxation and does not have an influence on the residual stress recovery during the cooling period as illustrated in Figure 16. Increasing the holding time provides higher stress relaxation, but improvement for addition 1 hour is less than 5 MPa.

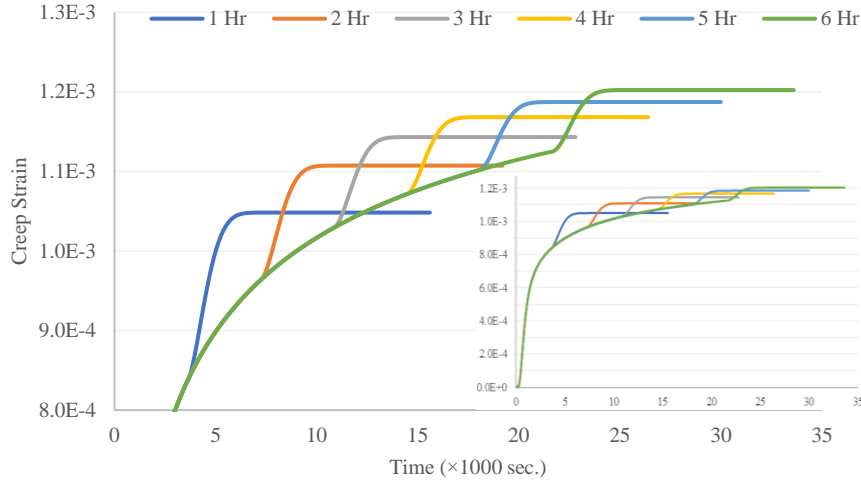


Figure 15. Time history of longitudinal creep strain at different holding times

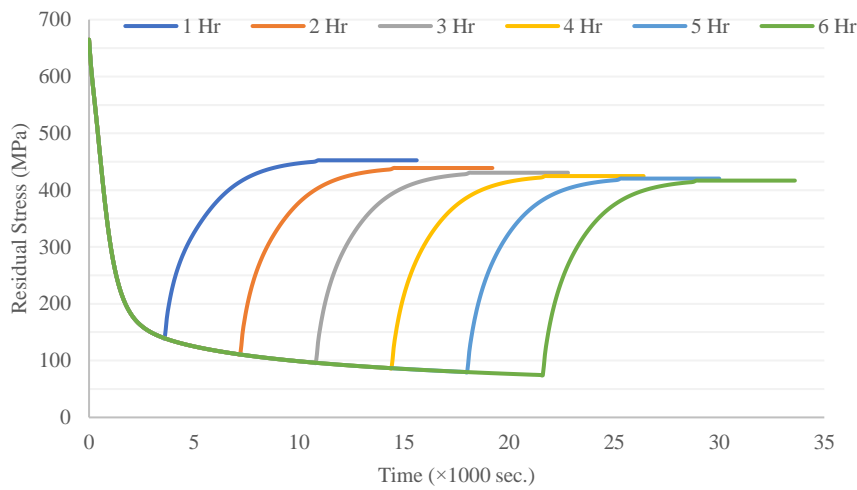


Figure 16. Time history of longitudinal residual stress at different holding times

## 6. CONCLUSION

We report the determination of optimum model parameters for the prediction of residual stress relaxation during post-weld heat treatment (PWHT) process in the bead-on-plate weldment of Inconel alloy 740H. The dominant mechanism of residual stress relief is the formation of creep strain during the PWHT process. The effect of ambient temperature and holding time of

the PWHT process were analysed by varying creep parameters to match experimental measurements. The results show that creep strain has a direct relation with the magnitude of stress relief. The results allow rational choice of the ambient temperature and hold time to maximize the creep strain to obtain the greatest stress relief. However, it is important to note that the relaxation process is accompanied by microstructural changes that may lead to crack formation, that must be the subject of specific study. The optimum PWHT ambient temperature and exposure time must be chosen using dual criteria of maximising creep strain and stress relaxation, whilst minimising the occurrence of creep-induced cracking. Furthermore, the cooling plan of the PWHT process must also be considered. The analysis of the holding time showed that increasing this parameter beyond a certain threshold does not have a significant effect on the magnitude of residual stress relief.

The proposed eigenstrain-creep model provided results that have good fit with experimental stress calculations. The bead-on-plate design has a complex nature. The weld beads are applied in a weld slot with a limited length. Welded and non-welded sections of the material have a complex interaction that determines the final residual stress state. After the success of the eigenstrain-creep model in a complex specimen, it can be stated that this model can be tested in all complex weld designs. The crucial point is careful selection of the functions that determine longitudinal distribution of weld bead. In this study, Knee function is used for this purpose, but different problems can need different functions.

## **ACKNOWLEDGEMENTS**

This project has received funding from the European Union's Horizon 2020 research and innovation programme under the Marie Skłodowska-Curie grant agreement No 794957 and

EPSRC through grant EP/S005072/1 Strategic Partnership in Computational Science for Advanced Simulation and Modelling of Engineering Systems (ASiMoV).

## REFERENCES

- [1] K. Nicol, Application and development prospects of double-reheat coal-fired power units Kyle, 2015. <https://doi.org/10.1007/s00223-016-0208-5>.
- [2] P.S.J. de Barbadillo J.J., Baker B.A., Gollihue R.D., Alloy 740H Component Manufacturing Development, in: Energy Mater. 2014, Springer, Cham, 2014: pp. 203–210.
- [3] S.J. Patel, J.J. De Barbadillo, B.A. Baker, R.D. Gollihue, Nickel base superalloys for next generation coal fired AUSC power plants, *Procedia Eng.* 55 (2013) 246–252. <https://doi.org/10.1016/j.proeng.2013.03.250>.
- [4] D.H. Bechetti, J.N. DuPont, J.J. de Barbadillo, B.A. Baker, M. Watanabe, Microstructural Evolution of INCONEL® Alloy 740H® Fusion Welds During Creep, *Metall. Mater. Trans. A.* 46 (2015) 739–755. <https://doi.org/10.1007/s11661-014-2682-6>.
- [5] Special Metals Corporation, Inconel Alloy 740H, (2017) 24. <http://www.specialmetals.com/assets/smc/documents/alloys/inconel/inconel-alloy-740-h.pdf> (accessed November 21, 2018).
- [6] H.H. Cerjak, Welding of steam turbine components, Study report of the COST 505 Welding Group, 1992.
- [7] M.E. Fitzpatrick, A. Lodini, Analysis of Residual Stress by Diffraction Using Neutron and Synchrotron Radiation, 2003. <https://doi.org/10.1088/0957-0233/14/9/703>.
- [8] M.E. Kartal, Y.H. Kang, A.M. Korsunsky, A.C.F.F. Cocks, J.P. Bouchard, The



- influence of welding procedure and plate geometry on residual stresses in thick components, *Int. J. Solids Struct.* 80 (2016) 420–429.  
<https://doi.org/10.1016/j.ijsolstr.2015.10.001>.
- [9] P. Palanichamy, M. Vasudevan, T. Jayakumar, Measurement of residual stresses in austenitic stainless steel weld joints using ultrasonic technique, *Sci. Technol. Weld. Join.* 14 (2009) 166–171. <https://doi.org/10.1179/136217108X394753>.
- [10] F. Uzun, A.N. Bilge, Ultrasonic Investigation of the Effect of Carbon Content in Carbon Steels on Bulk Residual Stress, *J. Nondestruct. Eval.* 34 (2015).  
<https://doi.org/10.1007/s10921-015-0284-x>.
- [11] F. Uzun, A.N. Bilge, Immersion ultrasonic technique for investigation of total welding residual stress, in: *Procedia Eng.*, 2011: pp. 3098–3103.  
<https://doi.org/10.1016/j.proeng.2011.04.513>.
- [12] K. Masubuchi, Models of Stresses and Deformation Due to Welding—A Review, *JOM J. Miner. Met. Mater. Soc.* 33 (1981) 19–23. <https://doi.org/10.1007/BF03339550>.
- [13] A.T. DeWald, M.R. Hill, Multi-Axial Contour Method for Mapping Residual Stresses in Continuously Processed Bodies, *Exp. Mech.* 46 (2006) 473–490.  
<https://doi.org/10.1007/s11340-006-8446-5>.
- [14] A.M. Korsunsky, *A Teaching Essay on Residual Stresses and Eigenstrains*, Butterworth-Heinemann, Oxford, United Kingdom, 2017.
- [15] G. Yan, A. Crivoi, Y. Sun, N. Maharjan, X. Song, F. Li, M.J. Tan, An Arrhenius equation-based model to predict the residual stress relief of post weld heat treatment of Ti-6Al-4V plate, *J. Manuf. Process.* 32 (2018) 763–772.  
<https://doi.org/10.1016/j.jmapro.2018.04.004>.
- [16] X. Cao, B. Rivaux, M. Jahazi, J. Cuddy, A. Birur, Effect of pre- and post-weld heat treatment on metallurgical and tensile properties of Inconel 718 alloy butt joints welded

using 4 kW Nd:YAG laser, *J. Mater. Sci.* 44 (2009) 4557–4571.

<https://doi.org/10.1007/s10853-009-3691-5>.

- [17] J. Cao, Y.F. Wang, X.G. Song, C. Li, J.C. Feng, Effects of post-weld heat treatment on microstructure and mechanical properties of TLP bonded Inconel718 superalloy, *Mater. Sci. Eng. A.* 590 (2014) 1–6. <https://doi.org/10.1016/j.msea.2013.10.013>.
- [18] D.W. Saunders, *Creep and relaxation of nonlinear viscoelastic materials*, 1978.  
[https://doi.org/10.1016/0032-3861\(78\)90187-8](https://doi.org/10.1016/0032-3861(78)90187-8).
- [19] D. Berglund, H. Alberg, H. Runnemalm, Simulation of welding and stress relief heat treatment of an aero engine component, *Finite Elem. Anal. Des.* 39 (2003) 865–881.  
[https://doi.org/10.1016/S0168-874X\(02\)00136-1](https://doi.org/10.1016/S0168-874X(02)00136-1).
- [20] H. Takazawa, N. Yanagida, Effect of creep constitutive equation on simulated stress mitigation behavior of alloy steel pipe during post-weld heat treatment, *Int. J. Press. Vessel. Pip.* 117–118 (2014) 42–48. <https://doi.org/10.1016/j.ijpvp.2013.10.008>.
- [21] P. Dong, S. Song, J. Zhang, Analysis of residual stress relief mechanisms in post-weld heat treatment, *Int. J. Press. Vessel. Pip.* 122 (2014) 6–14.  
<https://doi.org/10.1016/j.ijpvp.2014.06.002>.
- [22] B.L. Josefson, Residual Stresses and Their Redistribution During Annealing of a Girth-Butt Welded Thin-Walled Pipe, *J. Press. Vessel Technol.* 104 (1982) 245–250.  
<https://doi.org/10.1115/1.3264212>.
- [23] H. Alberg, D. Berglund, Comparison of plastic, viscoplastic, and creep models when modelling welding and stress relief heat treatment, *Comput. Methods Appl. Mech. Eng.* 192 (2003) 5189–5208. <https://doi.org/10.1016/j.cma.2003.07.010>.
- [24] A.H. Yaghi, T.H. Hyde, A.A. Becker, W. Sun, Finite element simulation of welded P91 steel pipe undergoing post-weld heat treatment, *Sci. Technol. Weld. Join.* 16 (2011) 232–238. <https://doi.org/10.1179/1362171810Y.0000000018>.

- [25] K.A. Venkata, S. Kumar, H.C. Dey, D.J. Smith, P.J. Bouchard, C.E. Truman, Study on the effect of post weld heat treatment parameters on the relaxation of welding residual stresses in electron beam welded P91 steel plates, *Procedia Eng.* 86 (2014) 223–233. <https://doi.org/10.1016/j.proeng.2014.11.032>.
- [26] F. Uzun, A.M. Korsunsky, On the identification of eigenstrain sources of welding residual stress in bead-on-plate inconel 740H specimens, *Int. J. Mech. Sci.* 145 (2018) 231–245. <https://doi.org/doi.org/10.1016/j.ijmecsci.2018.07.007>.
- [27] S. Russell, P. Norvig, *Artificial Intelligence A modern Approach*, Third Edit, Pearson Education Limited, n.d.
- [28] R. Quiza, O. López-armas, J.P. Davim, S.F. Wiesbaden, *Hybrid Modeling and Optimization of Manufacturing*, 2012.
- [29] D. Moens, D. Vandepitte, A survey of non-probabilistic uncertainty treatment in finite element analysis, *Comput. Methods Appl. Mech. Eng.* 194 (2005) 1527–1555. <https://doi.org/10.1016/j.cma.2004.03.019>.
- [30] V. Kobelev, Some basic solutions for nonlinear creep, *Int. J. Solids Struct.* 51 (2014) 3372–3381. <https://doi.org/10.1016/j.ijsolstr.2014.05.029>.
- [31] L. Bratke, L. Josefson, Estimation of Norton-Bailey parameters from creep rupture data, *Met. Sci.* 13 (1979) 660–664. <https://doi.org/10.1179/030634579790434312>.
- [32] J. Ahn, E. He, L. Chen, R.C. Wimpory, J.P. Dear, C.M. Davies, Prediction and measurement of residual stresses and distortions in fibre laser welded Ti-6Al-4V considering phase transformation, *Mater. Des.* 115 (2017) 441–457. <https://doi.org/10.1016/j.matdes.2016.11.078>.
- [33] M.B. Prime, Cross-Sectional Mapping of Residual Stresses by Measuring the Surface Contour After a Cut, *J. Eng. Mater. Technol.* 123 (2001) 162. <https://doi.org/10.1115/1.1345526>.

- [34] F. Uzun, J. Everaerts, L.R. Brandt, M. Kartal, E. Salvati, A.M. Korsunsky, The inclusion of short-transverse displacements in the eigenstrain reconstruction of residual stress and distortion in in740h weldments, *J. Manuf. Process.* 36 (2018) 601–612.  
<https://doi.org/10.1016/j.jmapro.2018.10.047>.
- [35] F. Uzun, A.M. Korsunsky, On the application of principles of artificial intelligence for eigenstrain reconstruction of volumetric residual stresses in non-uniform Inconel alloy 740H weldments, *Finite Elem. Anal. Des.* 155 (2019) 43–51.  
<https://doi.org/10.1016/j.finel.2018.11.004>.
- [36] T. Mura, *Mechanics of elastic and inelastic solids*, (1982). <https://doi.org/10.1007/978-94-009-3489-4>.
- [37] Y. Wang, J. Dong, M. Zhang, Z. Yao, Stress relaxation behavior and mechanism of AEREX350 and Waspaloy superalloys, *Mater. Sci. Eng. A.* 678 (2016) 10–22.  
<https://doi.org/10.1016/j.msea.2016.09.077>.
- [38] B.J. Foss, S. Gray, M.C. Hardy, S. Stekovic, D.S. McPhail, B.A. Shollock, Analysis of shot-peening and residual stress relaxation in the nickel-based superalloy RR1000, *Acta Mater.* 61 (2013) 2548–2559. <https://doi.org/10.1016/j.actamat.2013.01.031>.
- [39] J. Betten, *Creep mechanics* (Third Edition), 2008. <https://doi.org/10.1007/978-3-540-85051-9>.
- [40] F.H. Norton, *The Creep of Steel at High Temperatures*, McGraw-Hill Book Company, New York, 1929.
- [41] R.W. Bailey, The Utilization of Creep Test Data in Engineering Design, *Proc. Inst. Mech. Eng.* 131 (1935) 131–349.  
[https://doi.org/10.1243/PIME\\_PROC\\_1935\\_131\\_012\\_02](https://doi.org/10.1243/PIME_PROC_1935_131_012_02).
- [42] D.L. May, A.P. Gordon, D.S. Segletes, The Application of the Norton-Bailey Law for Creep Prediction Through Power Law Regression, Vol. 7A *Struct. Dyn.* (2013)

V07AT26A005. <https://doi.org/10.1115/GT2013-96008>.

- [43] J. Pelleg, Creep in Ceramics, Solid Mech. Its Appl. 241 (2017) 41–61.  
[https://doi.org/10.1007/978-3-319-50826-9\\_4](https://doi.org/10.1007/978-3-319-50826-9_4).
- [44] Y. Vetyukov, Modeling of Creep for Structural Analysis, Springer Vienna, Vienna, 2014. <https://www.springer.com/gb/book/9783540708346>.
- [45] C.Y. Jeong, S.W. Nam, J. Ginsztler, Activation processes of stress relaxation during hold time in 1Cr–Mo–V steel, Mater. Sci. Eng. A. 264 (1999) 188–193.  
[https://doi.org/https://doi.org/10.1016/S0921-5093\(98\)01086-7](https://doi.org/https://doi.org/10.1016/S0921-5093(98)01086-7).
- [46] A. Di Gianfrancesco, Materials for Ultra-Supercritical and Advanced Ultra-Supercritical Power Plants, Elsevier Ltd., 2017.  
<https://doi.org/https://doi.org/10.1016/B978-0-08-100552-1.00001-4>.
- [47] D.B. Fogel, The Advantages of Evolutionary Computation, in: BCEC, 1997.
- [48] M. Mitchell, An Introduction to Genetic Algorithms, The MIT Press, Cambridge, Massachusetts, 1998.
- [49] Y.C. Toklu, F. Uzun, Analysis of Tensegric Structures by Total Potential Optimization Using Metaheuristic Algorithms, J. Aerosp. Eng. 29 (2016) 4016023.  
[https://doi.org/10.1061/\(asce\)as.1943-5525.0000571](https://doi.org/10.1061/(asce)as.1943-5525.0000571).
- [50] F. Uzun, Form-finding of free-form tensegrity structures by genetic algorithm–based total potential energy minimization, Adv. Struct. Eng. 20 (2017) 784–796.  
<https://doi.org/10.1177/1369433216664739>.
- [51] F. Uzun, Form-finding and analysis of an alternative tensegrity dome configuration, Adv. Struct. Eng. 20 (2017) 1644–1657. <https://doi.org/10.1177/1369433216689570>.